Journal of Vacuum Science and Technology A

RESEARCH ARTICLE | JULY 01 2025

Combining molecular beam epitaxy and low-energy electron microscopy with *in situ* magnetic susceptibility measurements within an integrated ultrahigh vacuum system

Rongting Wu ; Ivan Bespalov ; Xi He ; Jin Zhao ; Shenglong Li; Ivan Božović

J. Vac. Sci. Technol. A 43, 042703 (2025)
https://doi.org/10.1116/6.0004699

JVST A
Journal of Vacuum Science & Technology A

ARTICLE

pubs.aip.org/avs/jva

Combining molecular beam epitaxy and low-energy electron microscopy with *in situ* magnetic susceptibility measurements within an integrated ultrahigh vacuum system

Cite as: J. Vac. Sci. Technol. A **43**, 042703 (2025); doi: 10.1116/6.0004699
Submitted: 6 May 2025 · Accepted: 6 June 2025 ·
Published Online: 1 July 2025

Rongting Wu,[1,2,a] Ivan Bespalov,[3,b] Xi He,[4] Jin Zhao,[3,c] Shenglong Li,[1,2] and Ivan Božović[3,4,5,a]

AFFILIATIONS

[1]State Key Laboratory of Semiconductor Physics and Chip Technologies, Institute of Semiconductors, Chinese Academy of Sciences, Beijing 100083, China
[2]Center of Materials Science and Optoelectronics Engineering, University of Chinese Academy of Sciences, Beijing 100049, China
[3]Energy Sciences Institute, Yale University, West Haven, Connecticut 06516
[4]Brookhaven National Laboratory, Upton, New York 11973
[5]Shanghai Advanced Research in Physical Sciences (SHARPS), Pudong, Shanghai 201203, China

[a]**Authors to whom correspondence should be addressed:** rtwu@semi.ac.cn and bozovic.hts@gmail.com
[b]**Present address:** Steele Laboratory, Department of Applied Physics and Materials Science, California Institute of Technology, Pasadena, CA 91125.
[c]**Present address:** Department of Physics, Emory University, Atlanta, GA 30322.

ABSTRACT

Quantum two-dimensional materials, including ultrathin superconducting films, are of great current research interest. These films are typically fabricated under ultra-high vacuum (UHV) conditions and are sensitive to the environment—prone to oxidation and contamination when exposed to the atmosphere. This hampers the study of their intrinsic properties by standard *ex situ* techniques. Here, we present a variable-temperature mutual inductance probe system integrated under UHV with molecular beam epitaxy (MBE) synthesis and low-energy electron microscopy, enabling nondestructive *in situ* characterization of superconducting thin films. The system employs a reflection-type configuration and reaches a low temperature (~4 K) using a high-cooling-power, vibration-isolated cryocooler. We demonstrate the system performance by measuring the superconducting critical temperature in a copper-oxide thin film.

I. INTRODUCTION

The superconducting state is distinguished by zero electrical resistivity and Meissner effect. Traditional resistivity measurement techniques, such as four-probe setups, usually require electrode fabrication, which may cause surface contamination and sample damage. For 2D quantum materials, which are of our focal interest, it is frequently also difficult to ensure a low enough contact resistance.[1,2] In contrast, magnetic probes can explore the properties of superconductors in a noncontact manner. Various magnetic measurement techniques, e.g., muon spin rotation (μSR),[3–6] microwave resonance,[7–10] and scanning superconducting quantum interference device (SQUID) susceptometry,[11–14] have been in use, but they often involve complex instrumentation or sample preparation processes. The mutual inductance (MI) technique stands out in its simplicity and convenience.[15,16] It allows for quantitative measurements of the key properties of the superconducting state, such as the critical temperature (T_c),[17–21] the magnetic penetration depth[22–30] (λ), and the critical current density (J_c).[31] However, most of the MI setups reported so far operate *ex situ*, requiring exposure of the sample to air, and are thus unsuitable for the study

of air-sensitive novel quantum 2D materials, such as ultrathin FeSe film, borophene, etc. One approach is to protect the surface with a capping layer on top, but this may obscure the intrinsic properties of the 2D superconducting film.

In this paper, we describe our design for a low-temperature MI system that enables accurate measurements of the critical temperature (T_c) in superconducting materials without exposing the sample to air. This MI system is integrated with a molecular beam epitaxy (MBE) system and a low-energy electron microscope (LEEM), allowing as-synthesized samples to be transferred under UHV from the MBE/LEEM chamber to the characterization chamber for diamagnetic measurements. We demonstrate the system performance by measuring T_c and various magnetic response properties of superconducting $La_{2-x}Sr_xCuO_4$ (LSCO) films. This choice was dictated by the fact that we have extensive experience with synthesizing highest-quality single-crystal LSCO thin films and characterizing them using the MI technique.[29,30] However, the synthesis of LSCO requires a high oxidation power, so the films that we used here as a calibration standard had to be synthesized in another (ozone-assisted) MBE system. After the synthesis, these films are characterized by another *ex situ* MI system first. Then, the calibration film was loaded into the new MBE/LEEM/MI system presented here and the film's T_c measured under UHV conditions. The resulting T_c was the same, proving that the new system works well and reliably. Thus, the present MBE/LEEM/MI system design overcomes the limitations of traditional techniques and provides a new tool for the discovery and study of novel superconducting materials.

II. RESULTS

A. LEEM/MI system development

Figure 1 shows the overall structure of the integrated MBE/LEEM/MI system. As depicted in Fig. 1(a), it consists of three interconnected ultra-high vacuum (UHV) chambers with a base pressure in the 10^{-10} Torr range. The preparation chamber is used for cleaning the sample surface by repetitive cycles of sputtering with noble gas ions and high-temperature annealing. The main chamber hosts a custom-built MBE synthesis system enhanced by real-time monitoring using a commercial LEEM (Elmitec GmbH LEEM III) apparatus.[32–35] In our custom-built MBE system, we can easily replace evaporation sources and crystal substrates as needed for experiments, enabling the growth of various 2D materials. For example, we use a boron (B) rod and an electron-beam evaporator (EFM 3, Focus GmbH) for the growth of borophene. The characterization chamber hosts a homemade low-temperature MI measurement system, highlighted by the red dashed rectangle. Both chambers are kept under UHV. A 130 cm long transfer arm enables sample transfer between the two chambers, in both directions. Integrating MBE and LEEM with the MI probe further

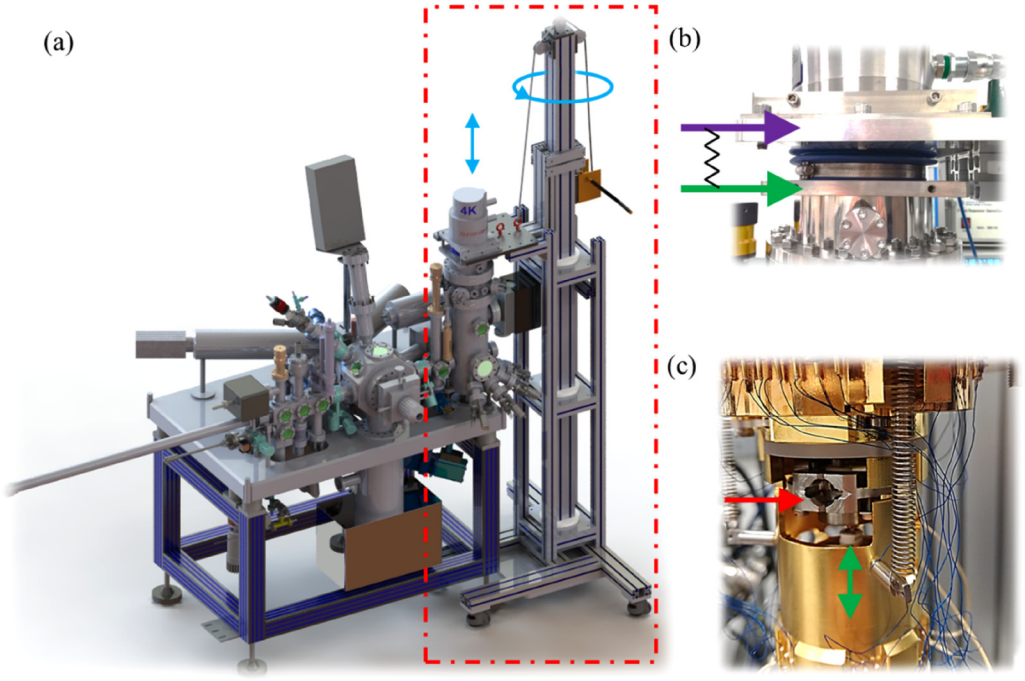

FIG. 1. Schematic diagram of the MBE/LEEM/MI system design. (a) The 3D sketch of the entire UHV system, containing an Elmitec LEEM III microscope and a homemade MI magnetic transport measurement system (red dashed rectangle). (b) A zoomed-in photo showing the connection between the vibration-isolated cryocooler (the top purple arrow) and the UHV chamber (the bottom green arrow) linked by soft rubber bellows. Helium gas fills the gap as the cooling medium. (c) A photo of the mutual-inductance probe head illustrates the process of transferring the LEEM sample holder (the top red arrow) and the movement of the probe (the bottom green arrow).

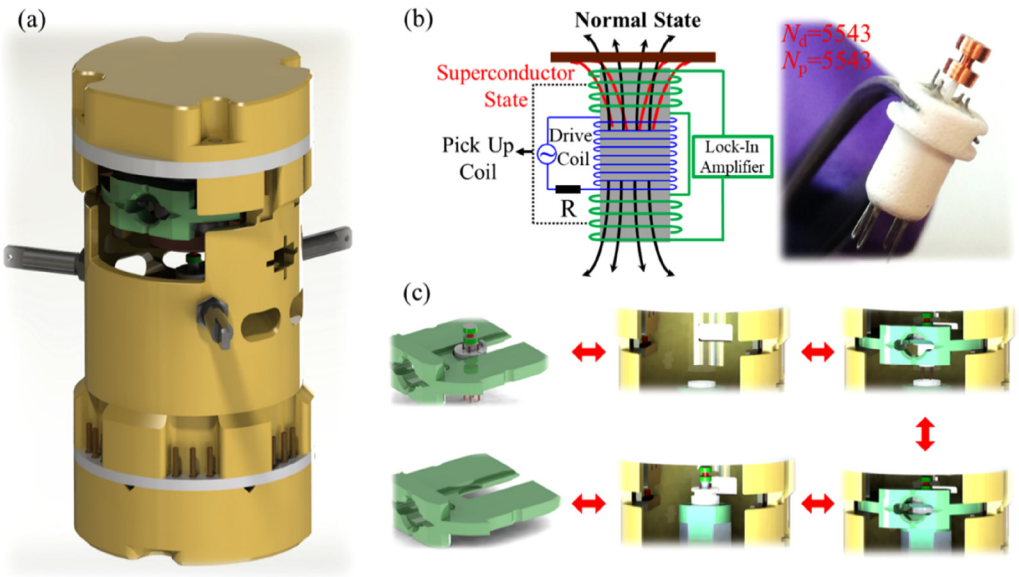

FIG. 2. Schematic diagram of the MI system. (a) The overall design of the MI head, which has the shape of a cylinder with a diameter of 42 mm and a height of 84 mm. (b) The schematic diagram of the reflection-type MI probe, which consists of three coils: a drive coil located in the center (the thin blue lines) generates a magnetic field (thicker dark arrows), and two pick-up coils with the same geometry and number of turns ($N_{p1} = N_{p2} = N_d = 5543$), but wound in opposite orientations, located on the two sides of the drive coil (medium green lines). (c) A schematic diagram illustrating the process of *in situ* switching of probes using a customized MI probe holder.

expands the system's capabilities, allowing for *in situ* investigation of the intrinsic magnetic responses of as-synthesized novel quantum 2D materials.

The MI system employs an ultralow vibration cryocooler, as shown in Fig. 1(b). The cryocooler (indicated by the top purple arrow) is mechanically supported by a homemade supporting stage with two degrees of freedom, allowing us to lift and rotate the cryocooler for maintenance. This support frame is isolated from the UHV chamber (the bottom green arrow) by flexible rubber bellows. In addition to the rubber bellows, a three-spring and magnetic-damping vibration isolation stage is added for enhanced mechanical stability. Helium gas is filled inside the rubber bellows as the cooling medium. This cryogenic setup can cool the system down to about 4 K, allowing for investigation of superconducting phenomena.

Figure 1(c) provides an enlarged view of the MI probe. The standard Elmitec LEEM sample holder (the top red arrow) is used with the sample facing down, enabling measurements of samples transferred from the MBE/LEEM chamber. The MI probe is located below the sample and driven by a Pan-type piezo-walker to approach and navigate on the sample surface for precise measurements of $l(T)$ and the superfluid density $n_s(T)$.

Figure 2(a) illustrates the overall structure of the MI head, featuring a compact cylindrical design with a diameter of 42 mm and a height of 84 mm. The head houses the MI probe, a standard LEEM sample holder, and an XYZ positioning stage enabling convenient sample navigation and measurements at precisely selected sample regions, orientations, and distances to the coils.

Figure 2(b) provides a schematic of our reflection-type MI probe. This type of MI probe, first proposed by Jeanneret *et al.*,[36] offers several advantages compared to the transmission-type MI systems.[37–39] The drive coil and pick-up coils are located on the same side of the sample, which makes the probe more compact and facilitates installation and maintenance. Our MI probe develops this idea further by including three coils, one drive coil (blue) placed symmetrically between two pickup coils (green). The drive coil, placed in the center, generates an up/down-symmetric magnetic field, as indicated by the dark arrows. The two pickup coils have identical geometry and number of turns ($N_{p1} = N_{p2} = N_d = 5543$) but are counter-wound. Thus, without a sample, or when a nonmagnetic thin film is in the normal state, equal but opposite induced voltages are generated in the two pick-up coils, resulting in a zero net output voltage. However, if a magnetically active sample is placed on one side, this distorts the magnetic flux lines closer to the sample, breaks the symmetry, and a nonzero differential voltage appears. One can think of this as an inductance bridge, designed to capture the differential signals. This system allows us to detect subtle changes in the magnetic field adjacent to the film, thus enabling sensitive measurements of the magnetic response.

The probe has five electrodes, with two for the drive coil, one each for the two pick-up coils, and the fifth one for additional desired applications (e.g., scanning tunneling microscopy, STM). The probe is mounted on a piezo-driven XYZ nano-positioning stage (FUTEC Corp.) with a range of $7 \times 7 \times 10\ \text{mm}^3$, so it can navigate on the sample surface and land on interesting areas with the assistance of an alignment camera. A customized probe holder is developed for *in situ* probe replacement, which enables smooth switching between different mutual inductance probes and a

six-point resistance probe,[35] and paves the way for future upgrading with other probes such as STM and atomic force microscopy, AFM. The probe-swapping process is illustrated in Fig. 2(c).

B. MI measurements on an LSCO film

MI measurements on an LSCO thin film were conducted to validate the system performance. The LSCO film, 20 nm thick, was grown on a $10 \times 10 \times 1$ mm^3 single-crystal $LaSrAlO_4$ (LSAO) substrate in another (ozone-assisted) MBE system, transferred *ex situ,* and outgassed for 8 h at 300 °C in the main chamber before measurements.

First, variable temperature performance was tested. Figure 3(a) illustrates the cooling-down dynamics of the cryocooler head (bottom blue line) and the sample stage (top red line). The liquid-helium-free Gifford–McMahon cryocooler can rapidly and economically reduce the sample temperature from room temperature to around 4 K in about 3.3 h. Figure 3(b) presents real and imaginary components of the MI voltage signals measured during the controlled warming-up and cooling-down processes. A driving current of 50 μA at 5 kHz and a ramping rate of 0.1 K/min was used. The offset of the warm-up and cooling-down MI measurement curves is only 0.1 K, indicating excellent thermal equilibration and the accuracy of temperature reading.

Notably, the values of real and imaginary voltages are one order of magnitude larger than those reported earlier for reflection-type MI systems.[40–42] Our miniature drive coil and pick-up coils were precisely wound using a 12.5 μm diameter wire by KUK Electronics AG in Appenzell, Switzerland. These coils have a large number of turns (5543), providing larger inductances, better sensitivity, and the ability to detect feeble magnetic responses.

Based on the data in Fig. 3(b), diamagnetic response information can be derived. At higher temperatures, the LSCO thin film behaves as a normal metal, and the real part of the MI remains nearly constant and small, indicating a weak magnetic response. As the temperature decreases and superconductivity emerges, the magnetic field inside the material is expelled due to the Meissner effect, and the real part of the MI signal shows a significant enhancement. The temperature at which the induced voltage undergoes a sudden increase corresponds to the onset of superconducting diamagnetism, identifying T_c of the sample. The presence of phase separation, if any, in the superconducting sample can be detected as the presence of multiple transition plateaus in the temperature dependence of the induced voltage. The magnitude of the induced voltage reflects the strength of the superconducting diamagnetism and allows one to calculate the magnetic susceptibility, $\lambda(T)$, the superfluid density $n_s(T)$, etc. The imaginary part shows a peak near T_c due to energy dissipation.[29,30,43] The onset of the dissipative peak coincides with zero DC resistivity, thus providing a precise, convenient, fast, contactless, *in situ* method of determining the actual $T_c(R = 0)$, which in this test sample is 29 ± 0.5 K.

Figure 4 illustrates the dependences of the MI signals in the LSCO thin film on frequency f [Fig. 4(a)] and amplitude I_d [Fig. 4(b)] of the driving current. At higher temperatures, the $\mathrm{Re}(V_p)$ signal is always small, due to compensation. Below T_c, $\mathrm{Re}(V_p)$ increases dramatically. The signal scales linearly with I_d except very near T_c, where some nonlinearities are indeed expected. The scaling with f is linear within some range ($f < 30$ kHz), indicating inductive excitation. At higher frequencies, nonlinear scaling emerges because dissipative excitation (such as eddy current in the metal parts around) starts to couple in. For simplicity, we just scaled all the signals to the value at one fixed temperature ($T = 23$ K), to compare them on equal footing. Note also that intrinsic, intensive properties of the material, such as T_c and λ, are defined assuming the thermodynamic equilibrium and the absence of any external perturbation, so strictly speaking, they correspond

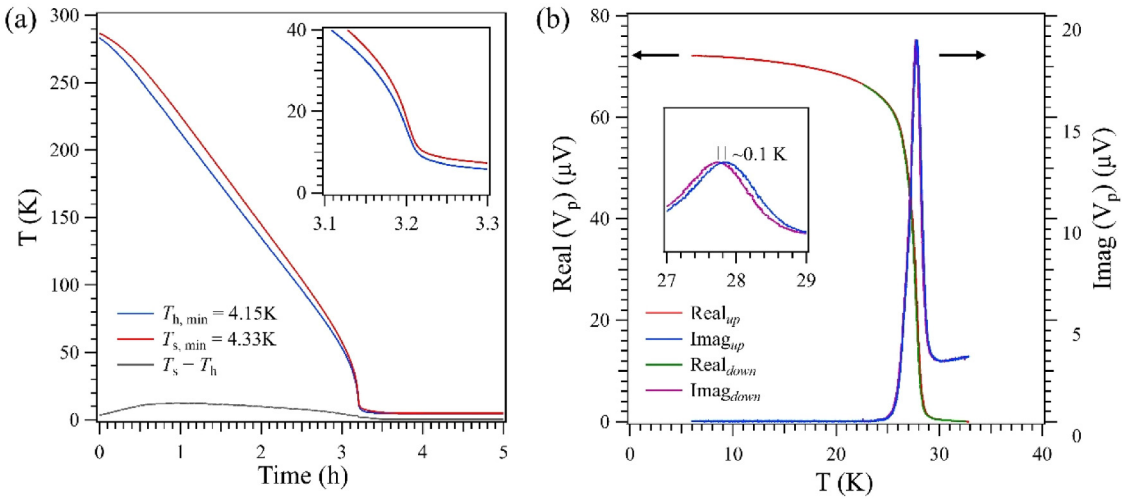

FIG. 3. MI measurement on the LSCO film. (a) Temperature vs time dependence of the cryocooler head (bottom, blue) and the sample stage (top, red) during rapid cooling progress. (b) The real and imaginary parts of the MI signal from the LSCO film during the warming up and cooling down processes, with a drive current of 50 μA and 5 kHz. The data show that the error in measuring the temperature is less than 0.1 K. Arrows next to the two curves point to the corresponding vertical scale on the left and right.

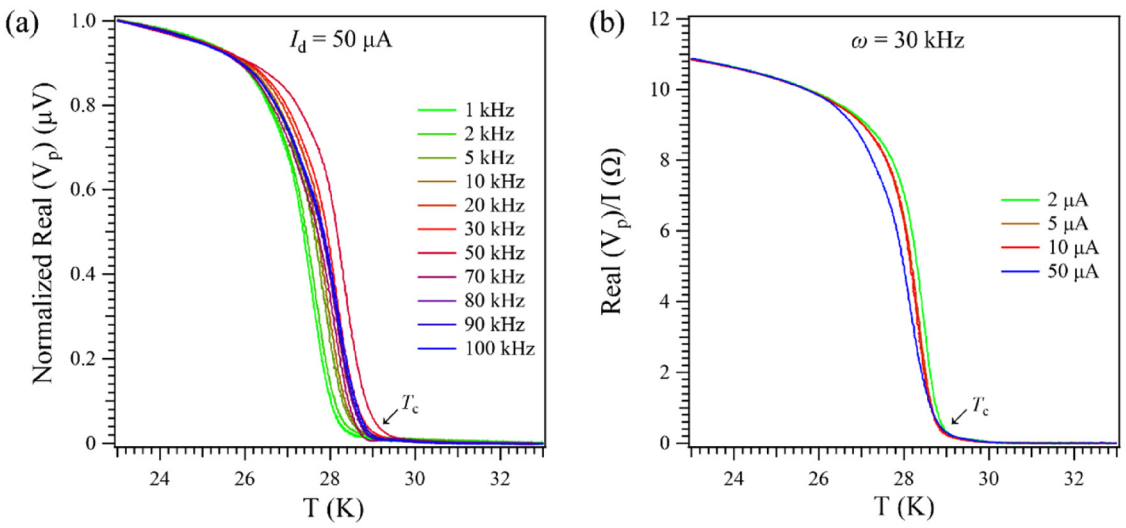

FIG. 4. Real part of the MI signal, Re(V_p), measured on the LSCO film at different currents and frequencies. (a) Re(V_p) measured at 50 μA alternating current at different frequencies, scaled to the value at T = 23 K. (b) Re(V_p) measured at 30 kHz frequency at different currents, scaled by the current amplitude. The signal onsets corresponds to the temperature T_c (R = 0).

to the limits $w \to 0$, $I_d \to 0$, as we explained in detail earlier.[30] We amply demonstrated[29,30] that T_c we infer in this way using MI is basically identical to the one we infer from DC resistivity measurements.

III. CONCLUSION

We present a report of a technical advance enabling the investigation of magnetic and superconducting properties of air-sensitive quantum materials. The new system component is an MI probe that employs a novel, compact, reflection, three-coil inductance-bridge design. The MI probe is combined with an XYZ nano-positioning stage, allowing for sample navigation and accurate magnetic response measurements. A Gifford–McMahon cryocooler with a vibration isolation design is used to enable continuous and economical low-temperature measurements. The probe functionality is illustrated by measuring T_c in an LSCO thin film.

This novel MI probe is integrated under UHV with MBE synthesis and real-time, nanometer-scale LEEM characterization of the film morphology and crystal structure. Altogether, this multimodule system offers a versatile platform for atomic layer-by-layer synthesis of 2D quantum materials and their comprehensive *in situ,* real-time analysis. Further development of the technology can include magnetic focusing to increase the spatial resolution, unlocking unprecedented research capabilities for the exploration of novel quantum materials.

IV. MATERIALS AND METHODS

Synthesis of a 20 nm LSCO thin film sample was performed on a $10 \times 10 \times 1$ mm^3 tetragonal LSAO substrate (MTI Corporation) using atomic-layer-by-layer molecular beam epitaxy (ALL-MBE) in a multichamber UHV apparatus.[43,44] The LSCO film was grown at a substrate temperature of 650 °C and a partial pressure of 5×10^{-6} Torr ozone. The thickness of the LSCO film was controlled *in situ* by using reflection high-energy electron diffraction (RHEED, STAIB Instruments GmbH) and monitoring the oscillations in the intensity of the specular reflection of the electron beam. After the growth, the LSCO film was annealed at the ozone partial pressure of 2×10^{-5} Torr for 30 min to compensate for oxygen vacancies, followed by cooling under the same pressure. After the growth, the sample was transferred to the LEEM-MI UHV system and outgassed under UHV conditions at 300 °C for 8 h.

The MI system uses a 1.1 W 4 K dry cryocooler (Advanced Research Systems, Inc.) for reaching cryogenic temperatures. Temperature was regulated using a cryogenic temperature controller (Model 335, Lake Shore Cryotronics, Inc.). The MI signal was measured by a lock-in amplifier (Model SR830, Stanford Research Systems Inc.) The real part of the MI signal shows a very sharp transition at T_c, because of the Meissner effect. The peak in the imaginary part near T_c originates from the changes in AC conductance due to superconducting fluctuations and vortex flow at the onset of the superconducting state.[45]

ACKNOWLEDGMENTS

LSCO films were synthesized and characterized at Brookhaven National Laboratory with support from the U.S. Department of Energy, Basic Energy Sciences, Materials Sciences and Engineering Division. The *in situ* inductance probe was designed, built, and attested at Yale University with support from the Gordon and Betty Moore Foundation's EPiQS Initiative through Grant No. GBMF9074. The data were analyzed, and the paper was written with support from the National Key R&D Program of China

(No. 2024YFA1410000), the National Natural Science Foundation of China (No. 62474172), and SHARPS.

AUTHOR DECLARATIONS

Conflict of Interest

The authors have no conflict of interest.

Author Contributions

Rongting Wu: Conceptualization (equal); Data curation (equal); Funding acquisition (equal); Investigation (equal); Methodology (equal); Project administration (equal); Supervision (equal); Validation (equal); Writing – review & editing (equal). **Ivan Bespalov:** Conceptualization (equal); Data curation (equal); Investigation (equal); Methodology (equal); Validation (equal); Visualization (equal); Writing – review & editing (equal). **Xi He:** Conceptualization (equal); Data curation (equal); Investigation (equal); Methodology (equal); Visualization (equal); Writing – original draft (lead); Writing – review & editing (equal). **Jin Zhao:** Data curation (equal); Investigation (equal); Methodology (equal); Validation (equal); Visualization (equal); Writing – original draft (lead); Writing – review & editing (equal). **Shenglong Li:** Conceptualization (equal); Data curation (equal); Formal analysis (equal); Investigation (equal); Methodology (equal); Software (equal); Writing – review & editing (equal). **Ivan Božović:** Conceptualization (equal); Data curation (equal); Formal analysis (equal); Funding acquisition (equal); Investigation (equal); Methodology (equal); Project administration (equal); Software (equal); Supervision (equal); Validation (equal); Writing – review & editing (equal).

DATA AVAILABILITY

The data that support the findings of this study are available from the corresponding authors upon reasonable request.

REFERENCES

[1]V. García-Vázquez, Neftalí Pérez-Amaro, A. Canizo-Cabrera, B. Cumplido-Espíndola, R. Martínez-Hernández, and M. A. Abarca-Ramírez, Rev. Sci. Instrum. **72**, 3332 (2001).
[2]S. Murase, K. Itoh, H. Wada, K. Noto, Y. Kimura, Y. Tanaka, and K. Osamura, Phys. C **357–360**, 1197 (2001).
[3]Y. J. Uemura *et al.*, Nature **364**, 605 (1993).
[4]C. Niedermayer, C. Bernhard, U. Binninger, H. Glückler, J. L. Tallon, E. J. Ansaldo, and J. I. Budnick, Phys. Rev. Lett. **71**, 1764 (1993).
[5]C. Panagopoulos, T. Xiang, W. Anukool, J. R. Cooper, Y. S. Wang, and C. W. Chu, Phys. Rev. B **67**, 220502 (2003).
[6]E. Morenzoni, B. M. Wojek, A. Suter, T. Prokscha, G. Logvenov, and I. Božović, Nat. Commun. **2**, 272 (2011).
[7]A. Hosseini, R. Harris, S. Kamal, P. Dosanjh, J. Preston, R. Liang, W. N. Hardy, and D. A. Bonn, Phys. Rev. B **60**, 1349 (1999).
[8]P. J. Turner *et al.*, Phys. Rev. Lett. **90**, 237005 (2003).
[9]R. Prozorov and R. W. Giannetta, Supercond. Sci. Tech. **19**, R41 (2006).
[10]D. M. Broun, W. A. Huttema, P. J. Turner, S. Özcan, D. C. Morgan, R. Liang, D. A. Bonn, and W. N. Hardy, Phys. Rev. Lett. **99**, 237003 (2007).
[11]M. E. Huber *et al.*, Rev. Sci. Instrum. **79**, 053704 (2008).
[12]B. Kalisky, J. R. Kirtley, J. G. Analytis, J.-H. Chu, A. Vailionis, I. R. Fisher, and K. A. Moler, Phys. Rev. B **81**, 184513 (2010).
[13]J. R. Kirtley *et al.*, Phys. Rev. B **85**, 224518 (2012).
[14]C. Herrera, J. Franklin, I. Božović, X. He, and I. Sochnikov, Phys. Rev. B **103**, 024528 (2021).
[15]A. F. Hebard and A. T. Fiory, Phys. Rev. Lett. **44**, 291 (1980).
[16]J. R. Clem and M. W. Coffey, Phys. Rev. B **46**, 14662 (1992).
[17]T. R. Lemberger, I. Hetel, A. Tsukada, and M. Naito, Phys. Rev. B **82**, 214513 (2010).
[18]T. R. Lemberger, I. Hetel, A. Tsukada, M. Naito, and M. Randeria, Phys. Rev. B **83**, 140507 (2011).
[19]W. H. Zhang *et al.*, Chin. Phys. Lett. **31**, 017401 (2014).
[20]Z. C. Zhang, Yi-Hua Wang, Qi Song, Chang Liu, Rui Peng, K. A. Moler, Donglai Feng, and Yayu Wang, Sci. Bull. **60**, 1301 (2015).
[21]J. F. Jia, Sci. Bull. **60**, 1368 (2015).
[22]A. T. Fiory, A. F. Hebard, P. M. Mankiewich, and R. E. Howard, Appl. Phys. Lett. **52**, 2165 (1988).
[23]A. Fuchs, W. Prusseit, P. Berberich, and H. Kinder, Phys. Rev. B **53**, R14745 (1996).
[24]J.-P. Locquet, Y. Jaccard, A. Cretton, E. J. Williams, F. Arrouy, E. Mächler, T. Schneider, O. Fischer, and P. Martinoli, Phys. Rev. B **54**, 7481 (1996).
[25]J. Y. Lee, Y. H. Kim, T.-S. Hahn, and S. S. Choi, Appl. Phys. Lett. **69**, 1637 (1996).
[26]J. H. Claassen, M. L. Wilson, J. M. Byers, and S. Adrian, J. Appl. Phys. **82**, 3028 (1997).
[27]R. F. Wang, S. P. Zhao, G. H. Chen, and Q. S. Yang, Appl. Phys. Lett. **75**, 3865 (1999).
[28]K. M. Paget, Sabyasachi Guha, Marta Z. Cieplak, Igor E. Trofimov, Stefan J. Turneaure, and Thomas R. Lemberger, Phys. Rev. B **59**, 641 (1999).
[29]I. Božović, X. He, J. Wu, and A. T. Bollinger, Nature **536**, 309 (2016).
[30]X. He, A. Gozar, R. Sundling, and I. Božović, Rev. Sci. Instrum. **87**, 113903 (2016).
[31]J. H. Claassen, M. E. Reeves, and R. J. Soulen, Rev. Sci. Instrum. **62**, 996 (1991).
[32]R. Wu, Ilya K. Drozdov, Stephen Eltinge, Percy Zahl, Sohrab Ismail-Beigi, Ivan Božović, and Adrian Gozar, Nat. Nanotechnol. **14**, 44 (2019).
[33]R. Wu, A. Gozar, and I. Božović, npj Quantum Mater. **4**, 40 (2019).
[34]R. Wu, Stephen Eltinge, Ilya K. Drozdov, Adrian Gozar, Percy Zahl, Jerzy T. Sadowski, Sohrab Ismail-Beigi, and Ivan Božović, Nat. Chem. **14**, 377 (2022).
[35]J. Zhao, Ivan Bespalov, Rongting Wu, and Ivan Božović, Rev. Sci. Instrum. **96**, 023907 (2025).
[36]B. Jeanneret, J. L. Gavilano, G. A. Racine, C. Leemann, and P. Martinoli, Appl. Phys. Lett. **55**, 2336 (1989).
[37]A. Gauzzi *et al.*, Rev. Sci. Instrum. **71**, 2147 (2000).
[38]V. A. Gasparov and I. Bozovic, Phys. Rev. B **86**, 094523 (2012).
[39]V. A. Gasparov, L. Drigo, A. Audouard, X. He, and I. Božović, Phys. Rev. B **94**, 014507 (2016).
[40]M. C. Duan *et al.*, Rev. Sci. Instrum. **88**, 073902 (2017).
[41]H. Nam, P.-H. Su, and C.-K. Shih, Rev. Sci. Instrum. **89**, 043901 (2018).
[42]M. Qin *et al.*, J. Supercond. Novel Magn. **33**, 159 (2020).
[43]C. Leemann, P. Lerch, G.-A. Racine, and P. Martinoli, Phys. Rev. Lett. **56**, 1291 (1986).
[44]X. He, X. Xu, X. Shi, and I. Božović, Condens. Matter **8**, 13 (2023).
[45]J. Wårdh, Mats Granath, Jie Wu, Anthony T. Bollinger, Xi He, and Ivan Božović, PNAS Nexus **2**, pgad255 (2023).